Supporting Information

Theoretical and Spectroscopic Evidence of the Dynamic Nature of Copper Active Sites in Cu-CHA Catalysts under Selective Catalytic Reduction (NH_3-SCR-NOx) Conditions

Reisel Millan,[1] Pieter Cnudde,[2] Alexander E.J. Hoffman, [2] Christian W. Lopes,[3] Patricia Concepción, [1] Veronique van Speybroeck,[,2] and Mercedes Boronat*[,1]*

[1] Instituto de Tecnología Química, Universitat Politècnica de València-Consejo Superior de Investigaciones Científicas, Avenida de los Naranjos s/n, 46022 València, Spain

[2] Center for Molecular Modeling, Ghent University, Technologiepark 46, 9052 Zwijnaarde, Belgium

[3] Laboratório de Reatividade e Catálise (LRC), Universidade Federal do Rio Grande do Sul, Bento Gonçalves Avenue 9500, 91501-970 Porto Alegre, Brazil

INDEX

1. Experimental section

1.1. Computational details

The Cu-SSZ-13 and Cu-SAPO-34 catalysts were modelled by means of a hexagonal unit cell containing 36 T and 72 O atoms. The two Al atoms substituting Si in SSZ-13 and the two Si atoms substituting P in SAPO-34 were located in the same 6-ring (*6r*), separated by one framework T atom. The two negative charges generated by this substitution were compensated with either two H^+ ions, one Cu^+ and one H^+ ion, or one Cu^{2+} ion, with the Cu^+ and Cu^{2+} ions being placed in the *6r* plane.

Static DFT calculations were performed at the PBE[S1] level of theory including Grimme's D3[S2] correction for dispersion interactions as implemented in VASP.[S3,S4] The valence density was expanded in a plane wave basis set with a kinetic energy cutoff of 600 eV, and the effect of the core electrons in the valence density was taken into account by means of the projector augmented wave (PAW) formalism.[S5] In all calculations the Brillouin zone was sampled at the gamma point. Electronic energies were converged to 10^{-6} eV and geometries were optimized until forces on atoms were less than 0.01 eV/Å. The positions of all atoms were allowed to relax in all geometry optimizations, keeping the volume and shape of the unit cell fixed. The vibrational frequencies were calculated on the optimized structures using density functional perturbation theory (DFPT).[S6] In these calculations only the Cu atom, the adsorbed molecules and all atoms in the *d6r* were included in the dynamical matrix. The intensities were derived with the help of the Born effective charge (BEC) tensor.[S7] However, this approach does not provide information about the bandwidth, so the spectra were generated by applying a Lorentzian line shape with full width at half-maximum (FWHM) of 10 cm^{-1}.

Ab initio Molecular Dynamics (AIMD) simulations were performed with the CP2K package[S8] at the revPBE-D3[S2, S9] level of theory. The Gaussian and plane waves (GPW)

method[S10] was used with the TZVP basis set for all atoms except Cu which was described with the DZVP-MOLOPT-SR-GTH basis set. A cutoff energy of 400 Ry was used for the auxiliary plane waves. Core electrons were represented with GTH pseudopotentials.[S11] Simulations were run in the NPT ensemble consisting of a production run of 50 ps for SSZ-13 and 100 ps for SAPO-34 after 10 ps of equilibration. Two temperatures were considered, 298 K and 523 K, controlled by a Nosé–Hoover chain thermostat[S12, S13] with three beads and a time constant of 300 fs. The pressure was set to 1 atm, controlled by a Martyna-Tobias-Klein barostat.[S14] The time step to integrate the equations of motion was set to 0.5 fs.

Vibrational frequencies were also calculated from AIMD simulations. The spectra were computed as the Fourier transform of the dipole autocorrelation function.[S15] This approach allows to take into account anharmonicities and finite temperature effects. The dipole moments were calculated every 2 fs using the Berry phase approach on the simulations carried out at 298 K and 1 atm.

1.2 Catalyst synthesis and characterization

Cu-SAPO-34 material was prepared by one-pot direct synthesis using a method developed by our group and described previously,[S16] from a synthesis gel of the following chemical composition: 0.19 SiO_2:0.5 Al_2O_3:0.4 P_2O_5:0.045 Cu-TEPA:0.855 DEA:18 H_2O (where DEA = diethylamine). The gel was introduced into an autoclave with a Teflon liner containing SAPO-34 seeds as well, and heated at 423 K under static conditions for 5 days. The resulting crystalline products were filtered and washed with water, dried at 373 K, and then calcined at 823 K in air to remove the occluded organic material. The chemical composition of the obtained materials was analyzed by ICP-OES (Varian 715-ES). The values obtained are (P+Al)/Si ratio = 8.1, Cu/Si ratio = 0.5 and 3.9 wt% Cu.

1.3. X-ray Absorption spectroscopy

The X-ray absorption spectroscopy experiments were performed at B18 beamline of Diamond Light Source (Didcot – UK). The sample of Cu-SAPO-34 was studied under different reaction conditions using a capillary reactor allowing operando studies. Cu K-edge XAS measurements were performed in transmission mode using a QEXAFS setup with a fast-scanning Si (111) double crystal monochromator. The time resolution of the spectra reported herein was 2.5 min/spectrum (kmax=15), on average four scans were acquired to improve the signal-to-noise level of the data for transmission measurements. All XAS spectra were acquired concurrently with the appropriate foil placed between I_t and I_{ref}. XAS data processing was performed using IFEFFIT with the DEMETER package (ATHENA and ARTEMIS programs).[S17] Spectra acquisition was performed at the following conditions: 1) at 298 K, after sample activation at 623 K in O_2 flow followed by He flow at 523 K; 2) at 353 K, 423 K and 523 K in the presence of NO and O_2 (2:5 molar ratio); 3) at 353 K, 423 K and 523 K in the presence of NO and NH_3 (2:0.5 molar ratio); 4) at 353 K, 423 K and 523 K in the presence of NO, NH_3 and O_2 (2:0.5:5) molar ratio. Linear Combination Fit (LCF) was performed to obtain the amount of Cu^+ and Cu^{2+} present in the catalyst at different reaction conditions. The standards of Cu^+ and Cu^{2+} were the spectra of sample during treatment with NO + NH_3 at 523 K and after activation in O_2 at 623 K, respectively. The energy interval used for LCF fitting was -5 to 15 eV, constraining the amount of Cu^+ and Cu^{2+} to be equal to 1 (fits without constraining were significantly close to 1). EXAFS data analysis was performed using the ARTHEMIS software, phase and amplitudes were calculated using the FEFF6 code. A corefinement approach was adopted allowing amplitude (coordination numbers), distances and Debye-Waller factor to vary and fixing one E_0 for each data set (e.g. spectra measured at the same reaction conditions).

1.4 Infrared spectroscopy

IR spectra were recorded with a Bruker spectrometer, Vertex 70, using a DTGS detector and acquiring at 4 cm^{-1} resolution. An IR cell allowing *in situ* treatments in controlled atmospheres and temperatures from 298 K to 773 K was connected to a vacuum system with gas dosing facility. For IR studies the samples were pressed into self-supported wafers and treated in O_2 flow for 2h at 623 K followed by vacuum (10^{-4} mbar) treatment at 423 K for 1 h or under dynamic vacuum (10^{-4} mbar) at 723 K for 1h. After activation, the sample was cooled down in vacuum to 298 K and submitted to calibrated reactant doses according to the experiment. Spectra were collected after each dosing and evacuation step. Thus, in the NH_3 adsorption experiment, $1.4*10^{-5}$ mol_{NH3} corresponding to a molar ratio of $2NH_3$/Cu was dosed at 298 K followed by increasing the temperature to 423 K and 523 K and subsequent sample evacuation (10^{-5} mbar) at 623 K. In the NO+O_2 experiments, NO ($1.4*10^{-5}$ mol) and O_2 ($3.1*10^{-5}$ mol), corresponding to a molar ratio 2NO/$5O_2$/Cu, were dosed at 298 K. Spectra were acquired at 298 K and at increasing temperatures of 423 K, 523 K and 623 K. In another set of experiment, after adsorption of 2NO/$5O_2$/Cu ($1.4*10^{-5}$ mol_{NO} and $3.1*10^{-5}$ mol_{O2}) at 423 K, NH_3 was added at the same temperature in controlled amounts, $0.7*10^{-5}$ mol_{NH3} and $1.4*10^{-5}$ mol_{NH3}, corresponding to molar ratios of $1NH_3$/Cu and $2NH_3$/Cu respectively. After spectra acquisition at 423 K, the temperature was increased to 523 K. In a final experiment, $1.4*10^{-5}$ mol_{NO} and $1.4*10^{-5}$ $mol_{NH3,}$ corresponding to molar ratios of 2NO/$2NH_3$/Cu, were added at 523 K. Subsequently $3.1*10^{-5}$ $mol_{O2,}$ corresponding to a molar ratio of $5O_2$/Cu was added. Spectra were acquired at 523 K after some time (i.e 30 min) and after increasing temperature to 573 and 623 K. The Orign software was used for spectra processing.

2. Mobility of Cu cations from ab initio molecular dynamics simulations

Table S1. Average distances between Cu^{+} or Cu^{2+} cations and the plane of the *6r* and root mean square deviations (RMSD) of the Cu^{+} or Cu^{2+} position with respect to the ensemble average obtained from AIMD simulations of Cu^{+} and Cu^{2+} cations in Cu-CHA catalysts interacting with O_2, NO, NO_2, and NH_3 at 298 and 523 K. Data obtained over 100 and 50 ps simulations for Cu-SAPO-34 and Cu-SSZ-13, respectively.

		d(Cu-*6r*)[a] (Å)				RMSD (Å)			
		Cu-SSZ-13		Cu-SAPO-34		Cu-SSZ-13		Cu-SAPO-34	
Cation	Adsorbate	298K	523K	298K	523K	298K	523K	298K	523K
Cu^{+}		0.30	0.31	0.51	0.48	0.30	0.44	0.30	0.47
Cu^{2+}		0.10	0.15	0.22	0.22	0.20	0.26	0.27	0.26
Cu^{+}	O_2	1.09	-	0.77	-	0.26	-	0.22	-
Cu^{+}	NO	1.82	1.98	0.83	0.86	0.52	0.45	0.32	0.47
Cu^{+}	2 NO	2.20	2.42	1.18	1.28	0.39	0.71	0.44	0.58
Cu^{+}	NO_2	1.60	1.67	0.53	0.65	0.29	0.38	0.28	0.44
Cu^{+}	2 NO_2	2.71	2.53	1.18	1.25	0.31	0.55	0.27	0.36
Cu^{+}	NH_3	2.40	2.60	1.38	0.98	0.39	0.66	0.29	1.08
Cu^{+}	2 NH_3	3.81	4.08	2.32	2.00	1.40	1.30	0.67	2.40
Cu^{2+}	O_2	0.11		0.23		0.19		0.21	
Cu^{2+}	ONO^{-}-NO_2	2.58	1.54	1.12	1.14	0.24	0.41	0.26	0.43
Cu^{2+}	NO-NO_3^{-}	1.91	2.24	1.07	1.23	0.23	0.45	0.36	0.53
Cu^{2+}	NO	0.51	0.24	0.32	0.39	0.32	0.37	0.25	0.36
Cu^{2+}	2 NO	0.66	0.74	0.96	0.46	0.25	0.38	0.36	0.40
Cu^{2+}	NH_3	0.65	-	0.37	0.39	0.40	-	0.26	0.44
Cu^{2+}	2 NH_3	1.53	1.53	0.97	0.97	0.36	0.51	0.40	0.46
Cu^{2+}	4 NH_3	4.36	4.28	2.00	2.06	0.27	0.39	0.30	0.47

Figure S1. (a) Snapshots of the interaction of Cu^{+} and Cu^{2+} cations in Cu-SSZ-13 with O_2, NO, NO_2, and NH_3 molecules and with nitrite and nitrate intermediates corresponding to geometries which are most frequently visited during AIMD runs of 50 ps at 298 K. (b) overview of the average distances between Cu^{+} or Cu^{2+} cations and the plane of the *6r* and root mean square deviations (RMSD) of the Cu^{+} or Cu^{2+} position with respect to the ensemble average at 298 K (blue) and 523 K (green) in each system. Al, O, Si, Cu, N, and H atoms depicted in gray, red, orange, green, blue, and white, respectively.

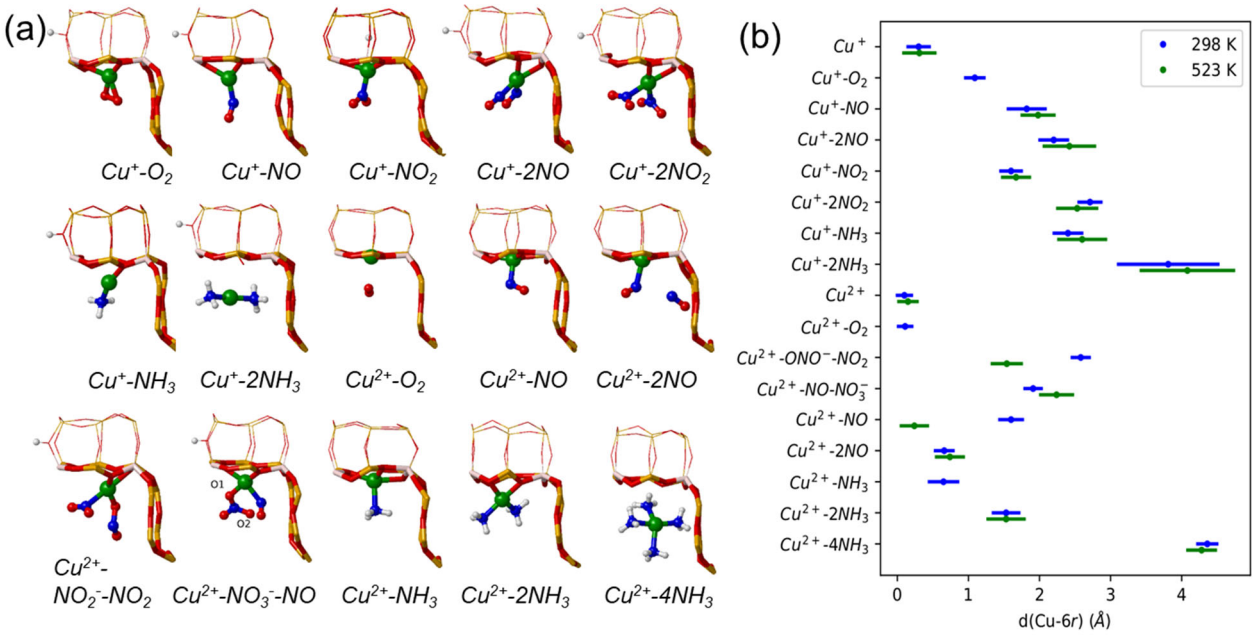

Figure S2. Evolution of Cu-O1 and Cu-O2 distances during AIMD simulations at 523 K for (a) Cu^{2+}-NO_2^--NO_2 and (b) Cu^{2+}-NO_3^--NO intermediates in Cu-SAPO-34.

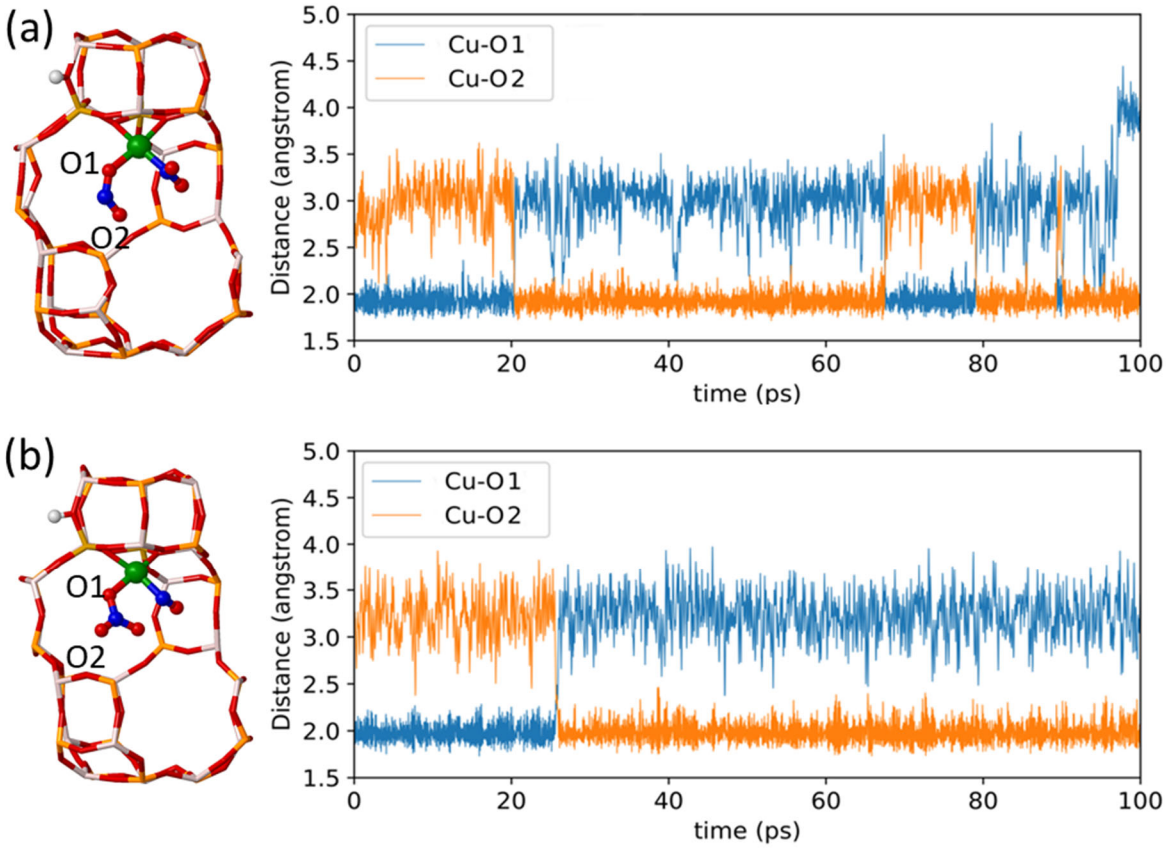

3. Vibrational spectra from static DFT and AIMD simulations

The IR spectrum of the parent H-SAPO-34 in the 800-1000 cm^{-1} region (Figure 3a) is nearly flat and only shows one small peak at 955 cm^{-1} associated to the bending mode of the proton of the Brönsted acid site. Accordingly, the simulated spectra of the neutral aluminophosphate AlPO and of H-SAPO-34 don't predict bands associated to framework T-O-T vibrations in this region (Figure 3b), and the calculated value for the OH bending frequency is slightly shifted to 1016 cm^{-1}. The IR spectrum of the Cu-SAPO-34 sample pre-activated in O_2 at 623 K and containing predominantly Cu^{2+} shows a peak at 964 cm^{-1} and an intense and broad band centered at ~885 cm^{-1} (Figure 3a, blue line), in agreement with previous studies on Cu-SSZ13.[S18-S20] These studies assigned a band at ~900 cm^{-1} to Cu^{2+} in the *6r*, and a peak at 950 cm^{-1} to $Cu(OH)^{+}$ species stabilized in the *8r*. However, no signal at ~3650 cm^{-1}, where the OH stretching vibration of $Cu(OH)^{+}$ should appear, is observed in the spectra of Figure S3, thus ruling out the presence of $Cu(OH)^{+}$ species in this sample. On the other hand, there is a very good agreement between the static and AIMD simulated spectra of Cu^{2+} in Cu-SAPO-34 (Figure 3b), both of them showing a peak at ~960 cm^{-1}, an intense band at ~890 cm^{-1} with a close feature at ~875 cm^{-1}, and a less intense peak at ~835 cm^{-1}. The correspondence between the static DFT and AIMD frequencies originates from the low mobility of Cu^{2+} cations, which are strongly bonded to the negatively charged oxygen atoms of the framework.

The IR spectrum of the same Cu-SAPO-34 sample pre-activated in vacuum at 723 K and containing predominantly Cu^{+} displays two less intense bands centered at ~850 and ~905 cm^{-1}, together with a shoulder at ~920 cm^{-1} (Figure 3a, red line). From static DFT calculations for the model containing Cu^{+}, three clear peaks are obtained at 983, 964 and 877 cm^{-1} (Figure 3b) associated to T-O-T vibrations in which only the oxygen atoms coordinated to Cu^{+} are involved. The AIMD spectrum is somewhat different, and shows

a group of bands centered around 910 cm^{-1} and another clear band at ~817 cm^{-1}. The difference between the static DFT and AIMD simulated spectra arises from the higher mobility of Cu^{+} in the *6r* of the Cu-SAPO-34 catalysts discussed in the main text, and points to a more reliable description of this dynamic system when using the molecular dynamics based approach. In such case, there is a very good agreement between theory and experiment regarding the band at ~905 cm^{-1}, while the IR band at ~850 cm^{-1} is clearly shifted to lower values.

Figure S3. IR spectra in the νOH region of the Cu-SAPO-34 sample (red line) after activation in O_2 flow for 2h at 623 K followed by vacuum treatment at 423 K for 1h. Marked in a rectangle the IR region where the νCu-OH vibration should appear. The bands at 3677, 3631 and 3594 cm^{-1} correspond to silanol and Brönsted acid sites which are also present in the IR spectra of H-SAPO-34 (blue line).

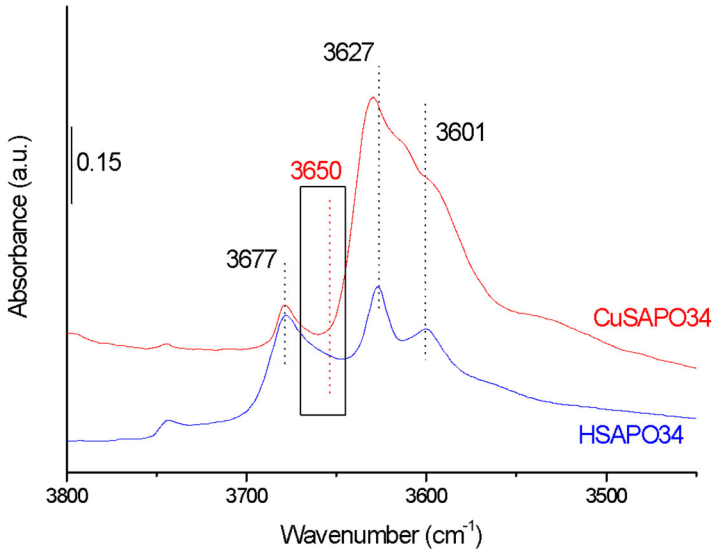

Figure S4. Vibrational frequencies in the 800-1000 cm^{-1} range calculated for Cu^{+} and Cu^{2+} cations interacting with O_2, NO, NO_2 and for Cu^{2+}-NO_3^--NO intermediate in Cu-SAPO-34 using static DFT calculations (red lines) and AIMD simulations at 298 K (green lines).

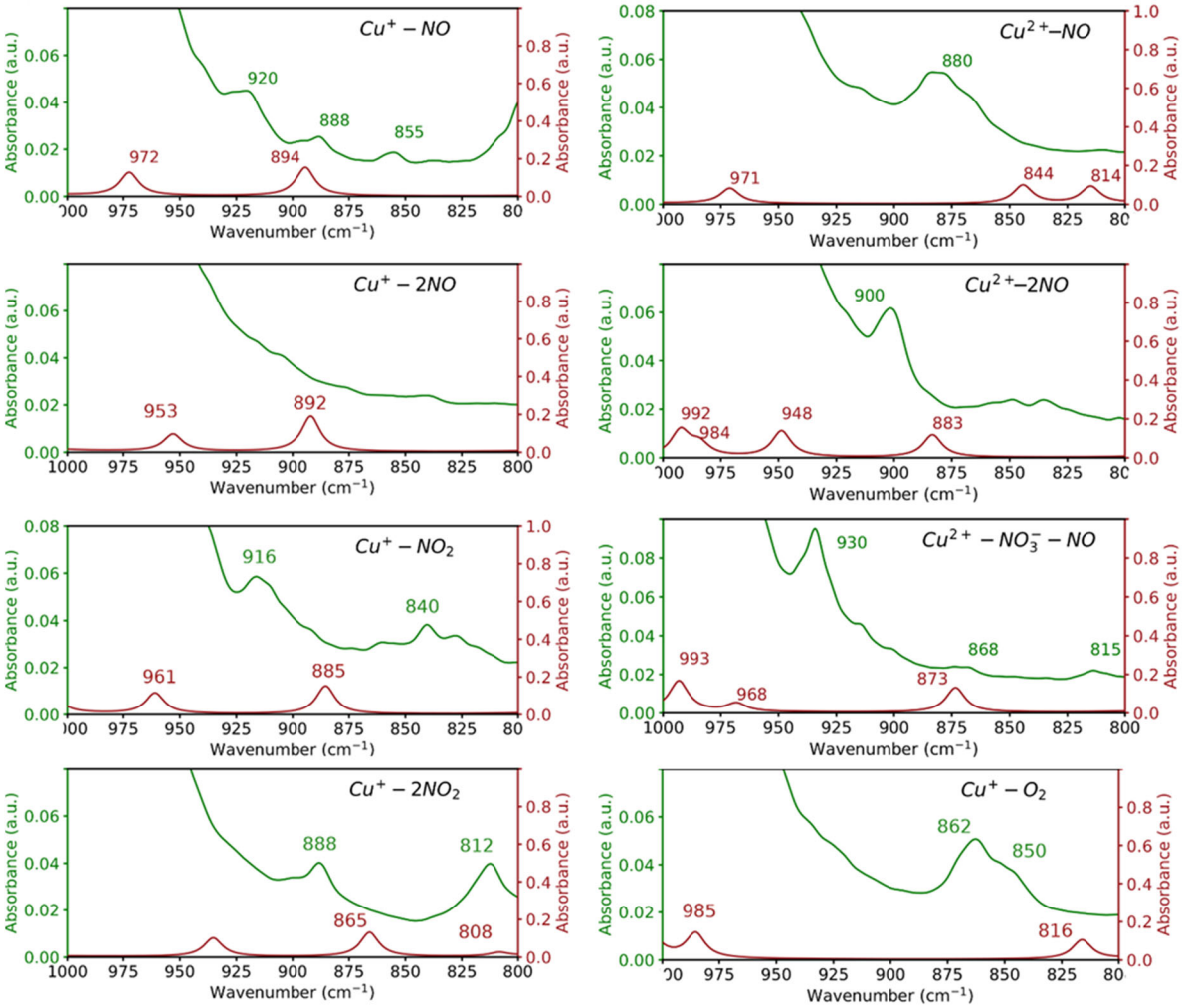

4. Characterization by XAS spectroscopy

When a Cu-SAPO-34 sample pre-activated in O_2 and containing preferentially Cu^{2+} is exposed to $2NO/0.5NH_3/Cu$ at 353 K, the XANES spectrum (Figure S5a) exhibits features at 8987, 8994 and 8998 eV characteristic of Cu^{2+} centers, and the typical edge-rising peak at 8983 eV indicating the presence of Cu^+.[S21] The relative amount of each oxidation state obtained from LCF (Linear Combination Fit) analysis is 65% Cu^{2+} and 35% Cu^+ (Table 2 and Figure S6d-f). At 423 K and 523 K the XANES spectra are dominated by the peak at 8983 eV typical of Cu^+, whose proportion has increased to 92% and 100%. The EXAFS spectra indicate that the coordination of copper changes from an average of three neighbors in the first coordination shell at 353 K to only two neighbors at a shorter distance of 1.88 Å at higher temperatures, pointing to the formation of $Cu^+(NH_3)_2$ species at 423 K (see fittings in Figure S7b and Table S2).

The XANES spectra of Cu-SAPO-34 in the presence of $2NO/5O_2/Cu$ (Figure S5c) show a weak pre-edge peak at ~8977 eV and two clear features at 8987 and 8998 eV characteristic of Cu^{2+} centers. According to the EXAFS spectra these Cu^{2+} cations are coordinated to the framework (see the well-defined second-shell peak at 2.3 Å in Figure S5d), and are directly bonded to four O atoms at 1.91 Å (Table 2) this coordination being stable in the whole range of temperature considered.

The XANES spectrum of Cu-SAPO-34 exposed to $2NO/5O_2/0.5NH_3/Cu$ (Figure S5e) changes significantly with temperature. At 353 K there is no contribution from Cu^+ and all Cu^{2+} is coordinated to framework oxygen atoms (Figure S5e,f and Table 2). At 423 K the reduction of Cu^{2+} to Cu^+ by reaction of NO with NH_3 starts to proceed. In the XANES spectra, the intensity of the signals at 8987, 8994 and 8998 eV decrease and a peak at 8983 eV appears, while in the EXAFS spectra the feature at 2.3 Å, indicative of a second coordination shell, disappears. Raising temperature to 523 K does not lead to significant

changes and the LCF analysis indicates a contribution of Cu^{+} of 65% at 423 K and 45% at 523 K (see Table 2), suggesting that larger amounts of NH_3 are necessary to reduce quantitatively Cu^{2+} in the presence of O_2.

Figure S5. Normalized XANES spectra at Cu K-edge (top) and |FT| of the k^2-weighted $\chi(k)$ functions (bottom) of Cu-SAPO-34 at different temperatures (353, 423 and 523 K) in presence of (a-b) $2NO + 0.5NH_3$, (c-d) $2NO + 5O_2$ and (e-f) $2NO + 0.5NH_3 + 5O_2$.

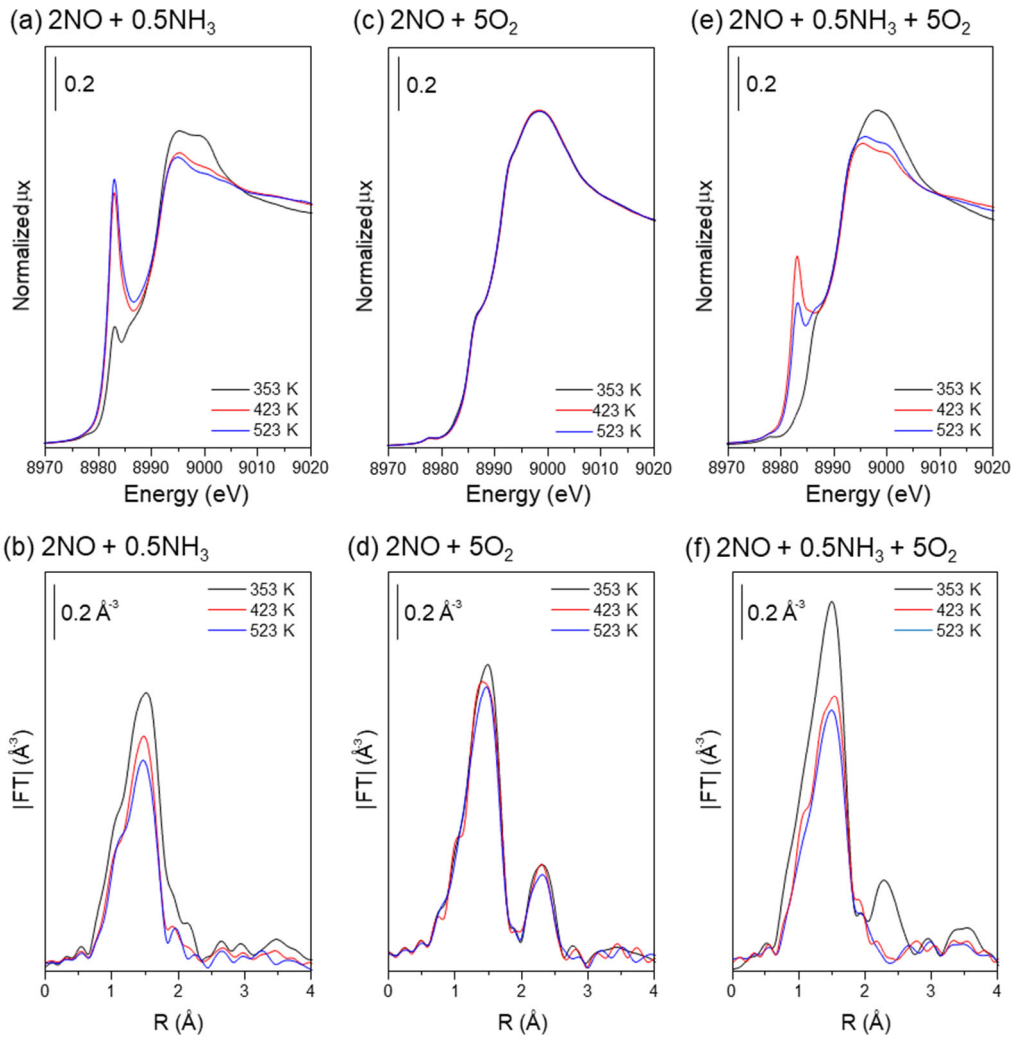

Figure S6. XANES spectra and Linear Combination Fit (LCF) analysis of Cu-SAPO-34 at different conditions: (a-c) $2NO+5O_2$, (d-f) $2NO+0.5NH_3$ and (g-i) $2NO+0.5NH_3+5O_2$ under increasing reaction temperature (353 → 423 → 523 K), respectively. The fit weights and the LCF residuals are also included in each plot. Spectrum of (f) represents the pure component for Cu^+.

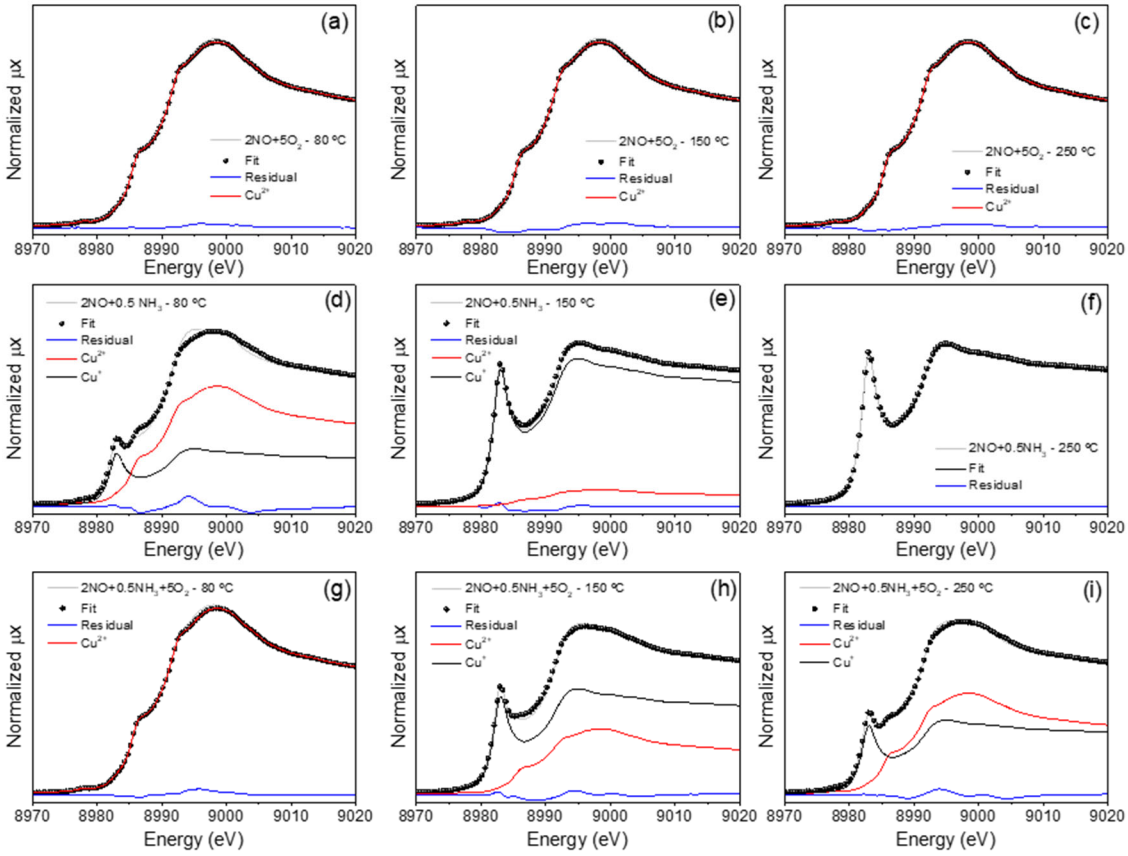

Figure S7. Curve-fittings and |FT| of the k^2-weighted $\chi(k)$ functions of Cu-SAPO-34 at different conditions: (a) $2NO+5O_2$, (b) $2NO+0.5NH_3$ and (c) $2NO+0.5NH_3+5O_2$ under increasing reaction temperature (353 (black) → 423 (red) → 523 K (blue)), respectively. Solid grey lines refer to experimental data while colored circles represent the fits.

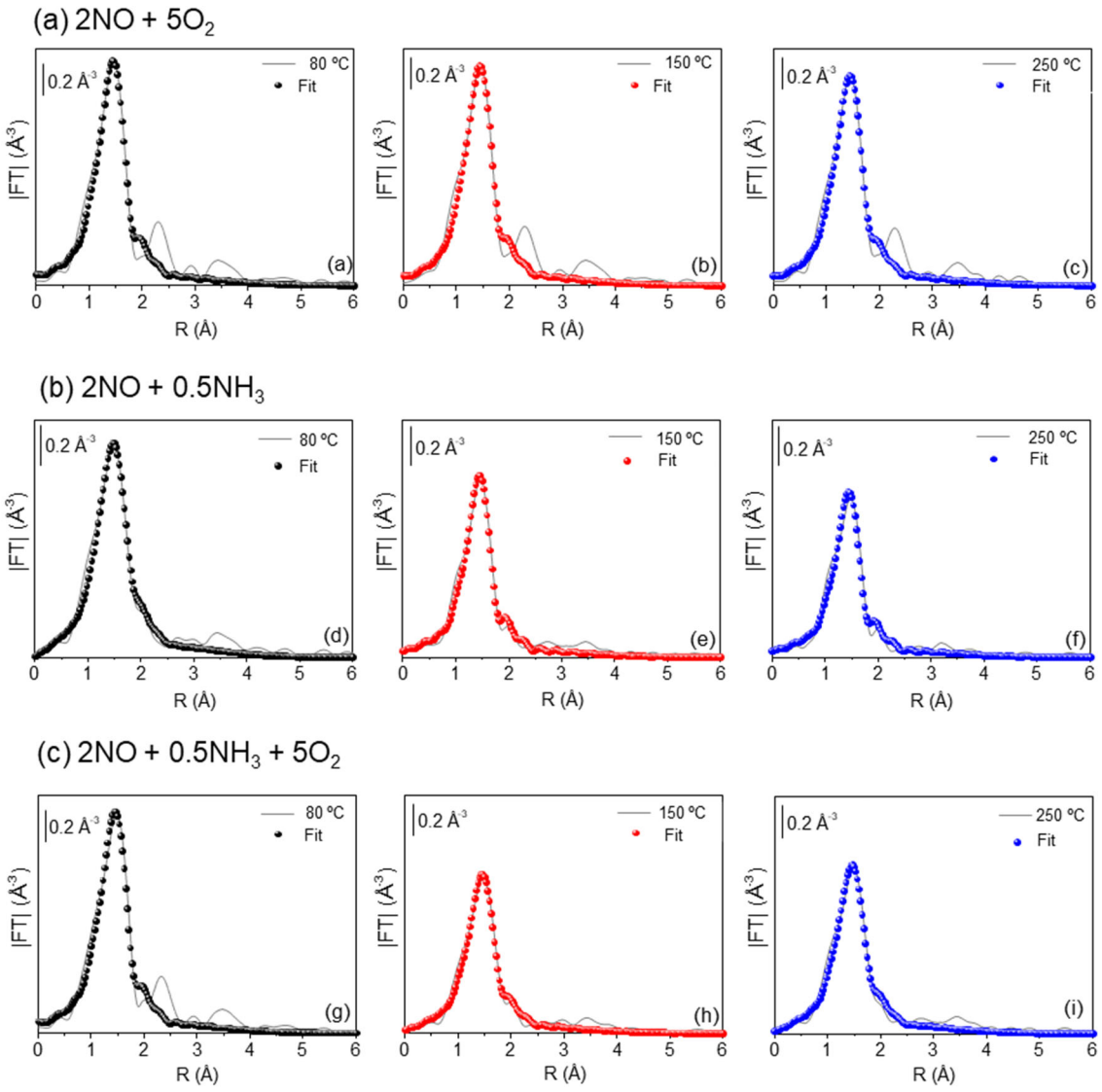

Table S2. Summary of obtained EXAFS fits of Cu-CHA at different reaction conditions.[a]

Condition	T (K)	N_{Cu-O}	R_{Cu-O} (Å)	$\sigma^2_{Cu-O(N)}$ (Å^2)	ΔE_0 (eV)	R-factor
Activation	523[b]	3.6 ± 0.4	1.910 ± 0.011	0.0090 ± 0.0018	-1.0 ± 1.2	0.0050
$2NO+5O_2$	353	3.9 ± 0.4	1.915 ± 0.006	0.0077 ± 0.0015	-0.2 ± 0.6	0.0085
	423	3.9 ± 0.5	1.912 ± 0.007	0.0081 ± 0.0019		0.0070
	523	3.9 ± 0.6	1.913 ± 0.009	0.0087 ± 0.0025		0.0064
$2NO+0.5NH_3$	353	3.2 ± 0.5	1.940 ± 0.014	0.0105 ± 0.0030	2.8 ± 1.2	0.0050
	423	1.7 ± 0.3	1.882 ± 0.012	0.0050 ± 0.0024		0.0091
	523	1.6 ± 0.5	1.879 ± 0.017	0.0053 ± 0.0042		0.0188
$2NO+0.5NH_3+5O_2$	353	3.6 ± 0.3	1.926 ± 0.007	0.0072 ± 0.0012	0.8 ± 0.7	0.0109
	423	2.5 ± 0.4	1.890 ± 0.009	0.0082 ± 0.0024		0.0141
	523	2.9 ± 0.5	1.902 ± 0.010	0.0094 ± 0.0030		0.0148

[a]A corefinement fit of the spectra was performed, fixing only one ΔE_0 value for each reaction condition; the fits were performed on the first coordination shell (ΔR = 1.0-2.0 Å) over FT of the k^2-weighted $\chi(k)$ functions performed in the Δk = 2.0-12.0 Å^{-1} interval. S_0^2 = 1.0. [b]Flowing He after treatment in O_2 at 623 K.

5. Characterization by IR spectroscopy

Figure S8. FTIR spectra of Cu-SAPO-34 (black line) after adsorption of $2NH_3$/Cu at 298 K (blue line) and increasing temperature to 423 K (green line) 523 K (pink line) and 623 K (red line). The insets show an amplification of the 800-1000 cm^{-1} region. Prior to adsorption the sample was pre-activated in vacuum at 723 K for 2 h.

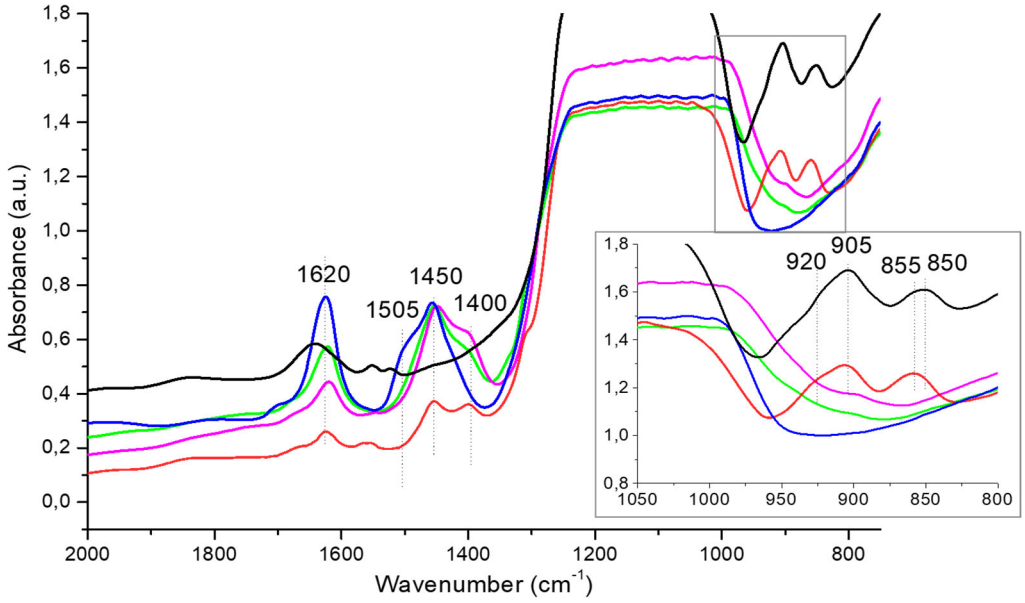

IR bands at 850 and 910 cm^{-1} associated to Cu^+ in the *6r* are clearly observed in the vacuum-activated sample before NH_3 adsorption (black line). After addition of $2NH_3$/Cu at 298 K (blue line), intense bands at 1620 cm^{-1} attributed to NH_3 adsorbed on Lewis acid sites and at 1450 cm^{-1} assigned to NH_4^+ cations on Brønsted acid sites, are detected. No IR bands are observed in the 800-1000 cm^{-1} region confirming the migration of Cu^+ to the cavity. When the temperature is raised to 423 K (green line) or 523 K (pink line) in the closed IR cell, the intensity of the 1620 cm^{-1} band decreases considerably, but the bands in the low frequency region characteristic of Cu^+ ions interacting with the zeolite framework in the *6r* are not yet restored. Only after vacuum at 623 K (red line) NH_3 is detached from Cu^+ ions and from the Brønsted acid sites and the bands at ~910 and ~850 cm^{-1} are recovered, indicating that Cu^+ ions have returned to their position in the *6r*.

Figure S9. FTIR spectra of (a) Cu-SAPO-34 (black line) after adsorption of 2NO/5O_2/Cu at 298 K (blue line) and (b) with increasing temperature at 423 K (green line), 523 K (pink line), and 623 K (red line). The insets show an amplification of the 800-1000 cm^{-1} region. Prior to adsorption the sample was pre-activated in O_2 at 623 K for 2 h, followed by vacuum at 423 K for 1 h.

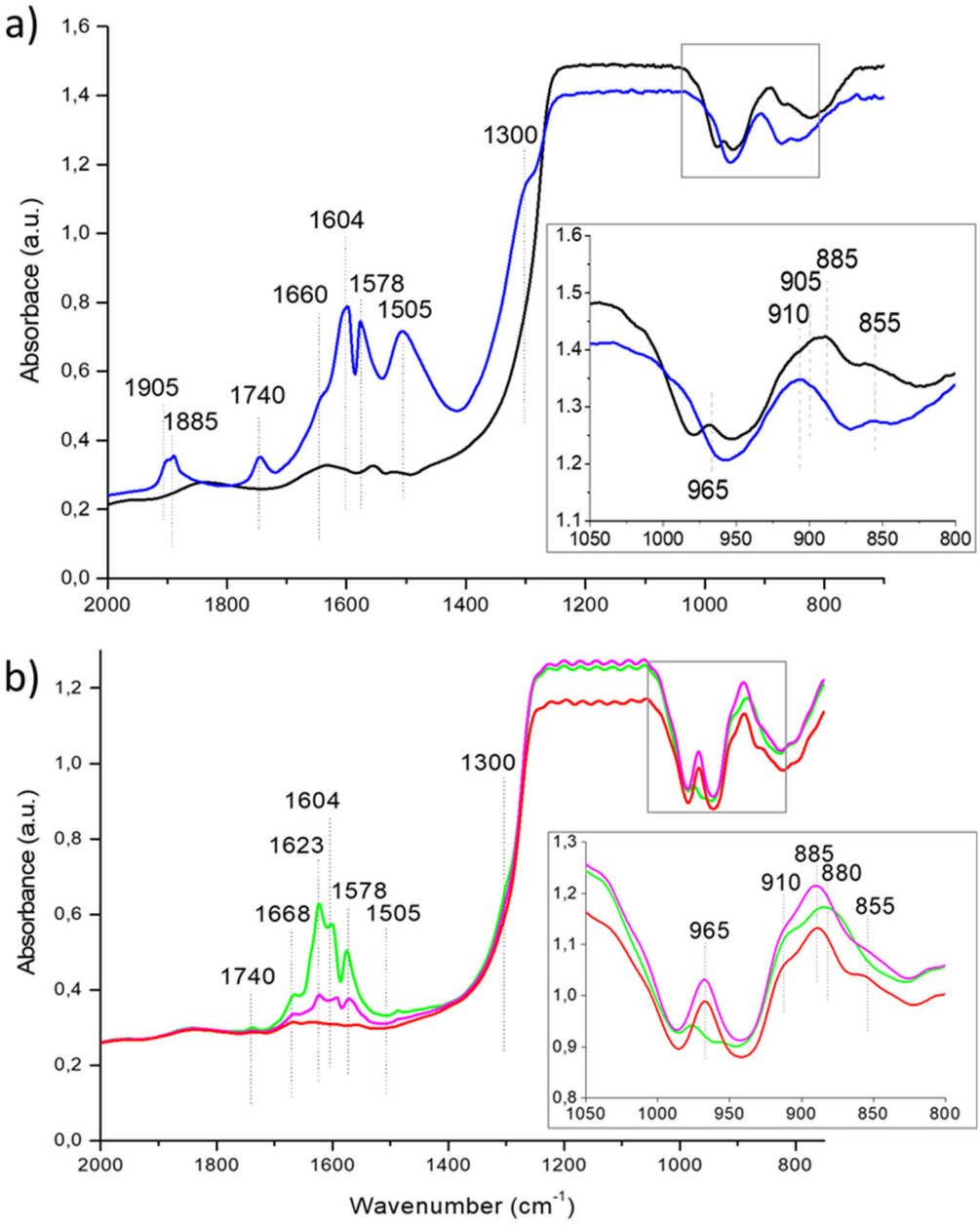

The IR spectrum of Cu-SAPO-34 sample pre-activated in O_2 (a, black line) exhibits lattice vibrational bands associated to Cu^{2+} (965 and 885 cm^{-1}) and Cu^{+} (910 and 855 cm^{-1}). After addition of $2NO/5O_2/Cu$ at 298 K (a, navy line), IR bands associated to NO_2 (1660 cm^{-1} physisorbed and 1604 cm^{-1} chemisorbed), nitrites (1300 and 1505 cm^{-1}), nitrates (1578 cm^{-1}), physisorbed N_2O_4 (1740 cm^{-1}) and NO interacting with Cu^{2+} (1905 and 1885 cm^{-1}) are observed in the high frequency region. Simultaneously, in the lattice vibrations frequency region, the IR peak at 965 cm^{-1} disappears, the signals at ~910 and 855 cm^{-1} decrease, and a broad band grows around 885 cm^{-1}. Based on the simulated spectra discussed in the main text, this broad band might include contributions from both Cu^{+} and Cu^{2+} interacting with NO_2, nitrites and nitrates (Table 1 in the main text). However, since the XAS study shows that only Cu^{2+} cations coordinated to the framework and directly bonded to four O atoms is present under these conditions (Table 2), the band is assigned to Cu^{2+} in the *6r* interacting with NO_2, nitrites and nitrates.

Raising temperature to 423 K (b, green line) leads to desorption of NO_2 (1660 cm^{-1}) and nitrites (1300 and 1505 cm^{-1}), and to reaction of nitrites with NO_2 to form NO and nitrates (1578 cm^{-1}). In this process, the intensity of the band at 880 cm^{-1} in the lattice vibrations region increases significantly. Raising temperature to 523 K (b, pink line) and 623 K (b, red line) results in desorption of all adsorbed species, as indicated by the disappearance of all bands between 1300 and 2000 cm^{-1}, and the recovering of the framework IR bands assigned to Cu^{2+} (965 and 885 cm^{-1}) and Cu^{+} (855 and 910 cm^{-1}) in the *6r*.

Figure S10. FTIR spectra of Cu-SAPO-34 after adsorption of 2NO/5O_2/Cu at 423 K (green line) followed by addition of 1NH_3/Cu (blue line) and 2NH_3/Cu (pink line) at 423 K and further increasing temperature to 523 K (red line). The insets show an amplification of the 800-1000 cm^{-1} region. Prior to adsorption the sample was pre-activated in O_2 at 623 K for 2 h, followed by vacuum at 423 K for 1 h.

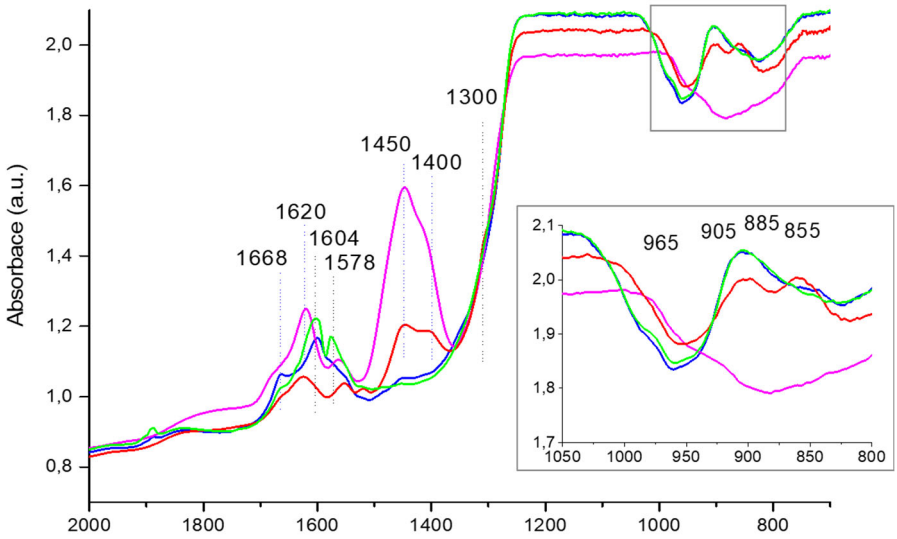

Starting from NO+O_2 adsorbed on Cu-SAPO-34 at 423 K (green line) controlled amounts of NH_3 were added without changing temperature. Addition of 1NH_3/Cu at 423 K (blue line) does not cause relevant changes in the spectrum, only a small increase in the intensity of the peak at 1668 cm^{-1} corresponding to physisorbed NO_2 and a slight decrease in the intensity of the peak at 1578 cm^{-1} assigned to nitrates. Under these conditions, the IR bands in the low frequency region are maintained, indicating that Cu^+ and Cu^{2+} cations remain coordinated to the framework oxygen atoms. In contrast, addition of 2NH_3/Cu at 423 K (pink line) causes the disappearance of all IR signals in the 800-1000 cm^{-1} region, supporting the XAS proposal that migration of Cu^+ cations from the *6r* to the cavity only occurs when there is enough NH_3 present in the reaction media. Simultaneously, intense bands associated to NH_4^+ cations (1450 cm^{-1}) and NH_3 bonded to Lewis sites (1620 cm^{-1}) are clearly observed in the high frequency region of the IR spectrum. Raising

temperature to 523 K (red line) facilitates the decomposition of all intermediate species present, as indicated by a clear decrease in the intensity of all bands in the high frequency region, while two broad bands centered at ~900 cm^{-1} and ~850 cm^{-1} appear again, indicating the reallocation of copper cations in the *6r* units of the SAPO-34 framework.

Figure S11. FTIR spectra of Cu-SAPO-34 after adsorption of $2NO/2NH_3/Cu$ at 523 K (black line) followed by addition of $5O_2/Cu$ at 523 K (blue line) and increasing temperature to 573 K (pink line) and 623 K (red line). The inset shows an amplification of the 800-1000 cm^{-1} region. Prior to adsorption the sample was pre-activated in O_2 at 623 K for 2 h, followed by vacuum at 423 K for 1 h.

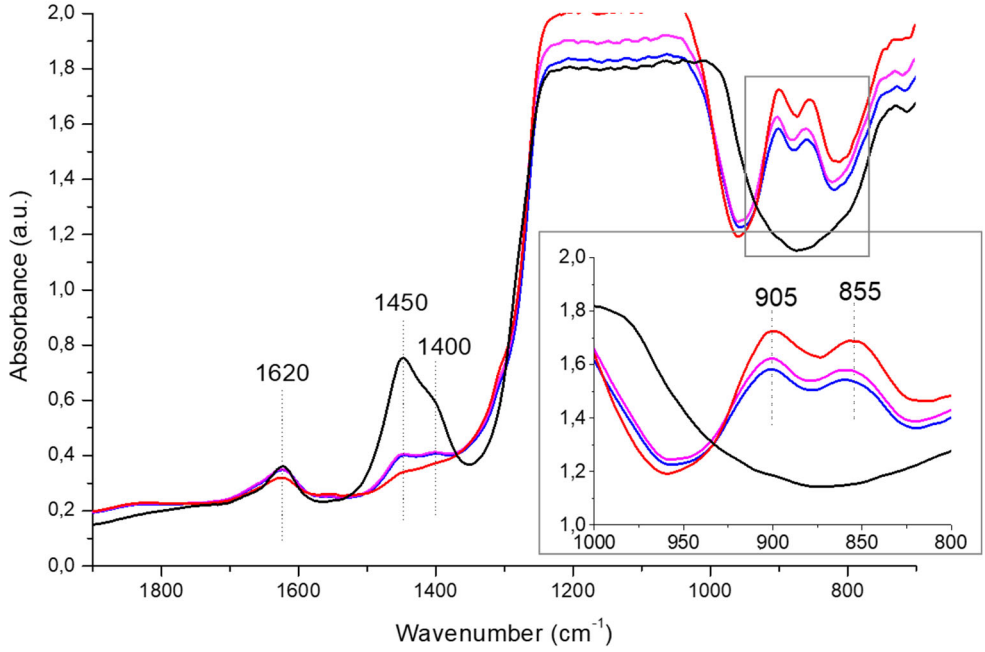

Finally, an additional experiment was done in which the Cu-SAPO-34 sample was first exposed to a reducing atmosphere consisting of $2NO/2NH_3/Cu$ at 523 K. Under these conditions all Cu^{2+} is reduced to Cu^{+} (Table 2) and the excess NH_3 ensures the total migration of Cu^{+} cations to the cavity in the form of $Cu^{+}(NH_3)_2$ complexes, as confirmed by the absence of IR bands in the 800-1000 cm^{-1} region (black line). After addition of

$5O_2$/Cu at 523 K (blue line) the bands centered at ~900 cm^{-1} and ~850 cm^{-1} appear, indicating a fast reaction of O_2 with NO and perhaps NH_3 that causes the return of copper cations to the *6r* of the SAPO-34 framework, while the NH_4^+ cations and NH_3 bonded to Lewis sites are consumed. Notice that no bands associated to nitrite or nitrate intermediates are ever observed, suggesting that their decomposition is fast at this temperature. Further increasing temperature to 573 K (pink line) and 623 K (red line) leads to desorption of all species and recovering of the broad bands at 880-910 cm^{-1} and ~850 cm^{-1} characteristic of a Cu-SAPO-34 catalyst containing Cu^+ and Cu^{2+} coordinated to framework oxygen atoms.

6. References

(S1) Perdew, J. P.; Burke, K.; Ernzerhof, M. Generalized Gradient Approximation Made Simple. *Phys. Rev. Lett.* **1996**, *77*, 3865–3868.

(S2) Grimme, S.; Antony, J.; Ehrlich, S.; Krieg, H. A Consistent and Accurate Ab Initio Parametrization of Density Functional Dispersion Correction (DFT-D) for the 94 Elements H-Pu. *J. Chem. Phys.* **2010**, *132*, 154104.

(S3) Hafner, J. Ab-Initio Simulations of Materials Using VASP: Density-Functional Theory and Beyond. *J. Comput. Chem.* **2008**, *29*, 2044–2078.

(S4) Kresse, G.; Furthmüller, J. Efficient Iterative Schemes for Ab Initio Total-Energy Calculations Using a Plane-Wave Basis Set. *Phys. Rev. B* **1996**, *54*, 11169–11186.

(S5) Blöchl, P. E. Projector Augmented-Wave Method. *Phys. Rev. B* **1994**, *50*, 17953–17979.

(S6) Baroni, S.; de Gironcoli, S.; Dal Corso, A.; Giannozzi, P. Phonons and Related Crystal Properties from Density-Functional Perturbation Theory. *Rev. Mod. Phys.* **2001**, *73*, 515–562.

(S7) King-Smith, R. D.; Vanderbilt, D. Theory of Polarization of Crystalline Solids. *Phys. Rev. B* **1993**, *47*, 1651–1654.

(S8) VandeVondele, J.; Krack, M.; Mohamed, F.; Parrinello, M.; Chassaing, T.; Hutter, J. Quickstep: Fast and Accurate Density Functional Calculations Using a Mixed Gaussian and Plane Waves Approach. *Comput. Phys. Commun.* **2005**, *167*, 103–128.

(S9) Zhang, Y.; Yang, W. Comment on ``Generalized Gradient Approximation Made Simple''. *Phys. Rev. Lett.* **1998**, *80*, 890–890.

(S10) Lippert, G.; Hutter, J.; Parrinello, M. The Gaussian and Augmented-Plane-Wave Density Functional Method for Ab Initio Molecular Dynamics Simulations. *Theor. Chem. Acc.* **1999**, *103*, 124–140.

(S11) Goedecker, S.; Teter, M.; Hutter, J. Separable Dual-Space Gaussian Pseudopotentials. *Phys. Rev. B* **1996**, *54* (3), 1703–1710.

(S12) Hoover, W. G. Canonical Dynamics: Equilibrium Phase-Space Distributions. *Phys. Rev. A* **1985**, *31*, 1695–1697.

(S13) Frenkel, D.; Smit, B. *Understanding Molecular Simulation: From Algorithms to Applications*; Elsevier Ltd, London, 2001.

(S14) Martyna, G. J.; Tobias, D. J.; Klein, M. L. Constant Pressure Molecular Dynamics Algorithms. *J. Chem. Phys.* **1994**, *101*, 4177–4189.

(S15) Thomas, M.; Brehm, M.; Fligg, R.; Vöhringer, P.; Kirchner, B. Computing Vibrational Spectra from Ab Initio Molecular Dynamics. *Phys. Chem. Chem. Phys.* **2013**, *15,* 6608–6622.

(S16) Martinez-Franco, R.; Moliner, M.; Concepcion, P.; Thogersen, J. R.; Corma, A. Synthesis, Characterization and Reactivity of High Hydrothermally Stable Cu-SAPO-34 Materials Prepared by "One-Pot" Processes. *J. Catal.* **2014**, *314*, 73–82.

(S17) Ravel, B.; Newville, M. ATHENA, ARTEMIS, HEPHAESTUS: Data Analysis for X-Ray Absorption Spectroscopy Using IFEFFIT. *J. Synchrotron Radiat.* **2005**, *12,* 537–541.

(S18) Kwak, J. H.; Varga, T.; Peden, C. H. F.; Gao, F.; Hanson, J. C.; Szanyi, J. Following the Movement of Cu Ions in a SSZ-13 Zeolite during Dehydration, Reduction and Adsorption: A Combined in Situ TP-XRD, XANES/DRIFTS Study. *J. Catal.* **2014**, *314*, 83–93.

(S19) Luo, J.; Gao, F.; Kamasamudram, K.; Currier, N.; Peden, C. H. F.; Yezerets, A. New Insights into Cu/SSZ-13 SCR Catalyst Acidity. Part I: Nature of Acidic Sites Probed by NH3 Titration. *J. Catal.* **2017**, *348*, 291–299.

(S20) Song, J.; Wang, Y.; Walter, E. D.; Washton, N. M.; Mei, D.; Kovarik, L.; Engelhard, M. H.; Prodinger, S.; Wang, Y.; Peden, C. H. F. et al. Toward Rational Design of Cu/SSZ-13 Selective Catalytic Reduction Catalysts: Implications from Atomic-Level Understanding of Hydrothermal Stability. *ACS Catal.* **2017**, *7*, 8214–8227.

(S21) Lomachenko, K. A.; Borfecchia, E.; Negri, C.; Berlier, G.; Lamberti, C.; Beato, P.; Falsig, H.; Bordiga, S. The Cu-CHA DeNO(x) Catalyst in Action: Temperature-Dependent NH3-Assisted Selective Catalytic Reduction Monitored by Operando XAS and XES. *J. Am. Chem. Soc.* **2016**, *138*, 12025–12028.